Available online at www.sciencedirect.com
ScienceDirect
Optik 117 (2006) 537–545
Optik Optics
www.elsevier.de/ijleo

Analysis of pupil and corneal wave aberration data supplied by the SN CT 1000 topography system

S.A. Comastri[a,b,*], G. Martin[a,c], T. Pfortner[d]

[a]*Laboratorio de Optica, Facultad de Ciencias Exactas y Naturales, Universidad de Buenos Aires, 1428 Buenos Aires, Argentina*
[b]*Consejo de Investigaciones Científicas y Técnicas, C1033AAJ Buenos Aires, Argentina*
[c]*QLOGIC S.A., Argentina and Instituto de Astronomía y Física del Espacio, (C1117ABE) Buenos Aires, (1428) Argentina*
[d]*Laboratorio Pfortner-Cornealent S.A., (C1119ACN) Buenos Aires, Argentina*

Received 9 August 2005; accepted 15 November 2005

Abstract

Ocular aberrations depend on pupil size and centring and the retinal image quality under natural conditions differs from that corresponding to laboratory ones. In the present article, pupil and wave aberration data supplied by the Shin Nippon CT 1000 (SN CT 1000) topography system are analysed. Two groups of eyes under natural viewing conditions are considered ((260 ± 20) lux at the eye under study). The first group consists of 10 normal eyes (-1.25 to 3 D sphere; 0 to -1.75 D cylinder) of five young subjects (age between 18 and 33 years). For this group, five determinations per eye are performed and the repeatability of results is analysed. Pupil centre is displaced from corneal vertex towards the temporal region, the largest displacement being (0.5 ± 0.1) mm. The variation of pupil diameter in each eye is less than 21% while the inter-subject variability is large since diameters are between (3 ± 0.3) and (5.3 ± 0.6) mm. Aberrations are evaluated for two different pupil sizes, the natural one and a fictitious one of 6 mm. The corneal higher-order root-mean square wavefront error (RMS_{HO}) for a 6 mm pupil centred in the corneal vertex, averaged across all eyes, is (0.37 ± 0.06) μm while, considering the natural pupil diameter, the average in each eye is significantly lower, up to eight times smaller. The fourth-order spherical aberration is an important aberration in the considered eyes, its maximum value for a 6 mm pupil being (0.38 ± 0.02) μm. The second group consists of 24 eyes of 12 subjects (age between 25 and 68 years) such that four eyes are of normal adults (1.25 to $+6$ D sphere; 0 to -0.5 D cylinder), eight have astigmatisms (-5.5 to $+3.25$ D sphere; -1.5 to -4.5 D cylinder), six have post-refractive surgery ($+0.5$ to $+3.5$ D sphere; -0.5 to -4 D cylinder) and six have keratoconus (-9.5 to $+1$ D sphere; -1 to -4.5 D cylinder). For this group only one determination per eye is performed. Pupil centre is displaced from corneal vertex towards the temporal region except in cases of keratoconus, where there can be a dominant upwards displacement. Pupil diameters are between 2.7 and 5.6 mm. The corneal higher order root mean square wavefront error for a 6 mm pupil ranges between 0.3 (normal eye) and 5.3 μm (keratoconus).

Keywords: Ocular pupil; Corneal aberrations

1. Introduction

The perceived image quality [1,2] depends on the performance of both the optical and the neural systems

*Corresponding author. Laboratorio de Optica, Facultad de Ciencias Exactas y Naturales, Universidad de Buenos Aires, 1428 Buenes Aires, Argentina.
E-mail address: comastri@df.uba.ar (S.A. Comastri).

0030-4026/$ - see front matter © 2006 Elsevier GmbH. All rights reserved.
doi:10.1016/j.ijleo.2005.11.018

and is affected by factors such as diffraction, intraocular scattering; veil luminance, colour dispersion, Stiles–Crawford effect, limits imposed by the size and spacing of photoreceptors and the subject's psycho-physical state. Wavefront aberration [3–8] is one of the important factors affecting retinal image quality and eyes can suffer not only from conventional or lower-order aberrations but also from higher order ones [9–29], specially in old normal or abnormal subjects even with small pupils and in young subjects with large pupils [14]. Ocular aberrations are usually evaluated by tracing rays and describing the wavefront aberration as a superposition (up to a convenient order) of Zernike polynomials. The rays traced to evaluate aberrations of the complete eye (cornea–pupil–crystalline lens) are real and methods such as Shack–Hartmann sensor, laser ray tracing, etc., are employed [20–23]. The rays traced to evaluate corneal aberrations are virtual considering the corneal profile supplied by topography systems [16–19] and some of these, for e.g., Keratron, OPD Nidek, KR-9000 PW de Topcon, and Skin Nippon CT 1000 (SN CT 1000), yield both topographic and corneal aberrometric data. On studying aberrations introduced by the complete eye and by the cornea, it has been found that in normal eyes there is often a partial compensation between higher-order aberrations introduced by the anterior corneal face and by the internal optics [11,21], while in cases of corneal pathologies this compensation is reduced [13,16–19,24]. The analysis of higher-order ocular aberrations is of interest principally to evaluate optical quality of eyes before and after refractive surgery [20,21], to improve the optical design of ophthalmic, contact or intraocular lenses [25] and to design aberration compensation systems for studying microscopic retinal structures [29].

Higher-order aberrations and, consequently, the corresponding root-mean-square wavefront error (RMS_{HO}), are affected by both size and centring of the pupil [14,17–21,26]. Frequently [9,17,19–21], aberrations are evaluated under laboratory conditions (paralysed accommodation, pupil dilated with drug and artificial pupil) and the results obtained yield valuable information, though they do not precisely account for visual performance in everyday life [1,2,10,17,24,26]. It has been reported [12] that the difference in retinal image quality between the young and old found under laboratory conditions decreases under natural ones. For a given illumination, each subject has a particular pupil diameter and, additionally, the eye disposes of mechanisms to improve vision such as slight changes in pupil size to optimise accommodation, frowning to trim the pupil reducing aberrations, blinking to modify the tear film and brain image processing to extract useful information present in the image [17] .

In this article, we analyse data supplied by the SN CT 1000 topography system developed at the Laboratorio Pfortner-Cornealent-Argentina. Besides rendering topographic data, this device records the image of the ocular pupil, yielding the value in mm of both its diameter and the displacement of its centre from the keratometric axis. This system computes corneal aberrations, considering the corneal vertex as the origin of the coordinates system, tracing virtual rays through the corneal profile and describing the wavefront aberration as a Zernike expansion of up to 7th order. We consider two groups of eyes. The first group is composed of 10 normal eyes (two requiring no refractive correction and three requiring spherical correction less than 3 D and cylindrical less than 1.75 D) of five young subjects (age between 18 and 33 years). For this group we study the repeatability of the data recording five topographies per eye. We study the variation of size and centring of the pupil under natural viewing photopic conditions both in each eye and among eyes. For two values of pupil diameter, the natural one of each eye and a fixed value of 6 mm for every eye, and considering RMS_{HO} as a global optical quality metric, we analyse its variability for each eye and between eyes, and the consequences of considering a natural or a 6 mm pupil. The second group consists of 24 eyes of 12 subjects (age between 25 and 68 years) such that four eyes are of two normal adults (51 and 52 years old), eight are astigmatic, six have post-refractive surgery and six have keratoconus. For this group, we perform only one determination per eye, we analyse the values of pupil diameters and the displacement of the pupil centre from the corneal vertex and we calculate the corneal RMS_{HO} for a 6 mm pupil.

2. Aberrations and ocular pupil

Assuming monochromatic illumination, we summarise some concepts related to the aberrations and the pupil.

2.1. Wavefront aberration and its expansion in Zernike polynomials

For any image-forming system [3–8], we consider cartesian coordinates (ξ,η) and (ξ',η') in the object and image planes, cartesian coordinates (X, Y) and (X', Y') in the reference spheres at the entrance and exit pupils respectively, and, at image space, we take into account a convenient axis termed z' (Fig. 1). For an object point Q, the intersection of the principal ray with the paraxial image plane can be chosen a priori as a reference image point and we denote it Q'. A ray from Q which is not the principal one intersects the image plane at a point termed P', the exit pupil reference sphere (of radius $R' = E'Q$) at B' and the real wavefront at K'. The wavefront aberration, $W(X', Y')$, is the optical path length along the ray from the exit pupil reference sphere

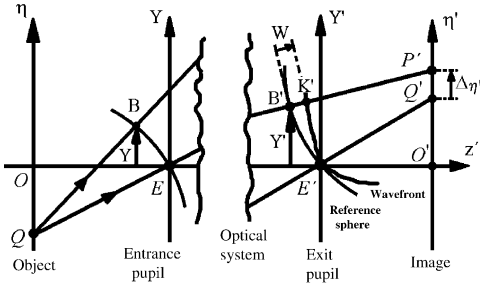

Fig. 1. Coordinates in the object, image and pupils planes. Q and Q' are an object point and its ideal image point while E and E' are points at the entrance and exit pupils centres; respectively, $QEE'Q'$ is the principal ray and $QBB'Q'$ is an arbitrary ray.

to the real wavefront, while OPD is the optical path length difference along the ray from Q to the real wavefront and from Q to the ideal wavefront; so, if square brackets indicate optical path length, $W(X',Y') = [B'K'] = [QE']-[QB'] = -\mathrm{OPD}$ (with $W(X',Y')>0$ in Fig. 1). If the refraction index in the image space is termed n', the wavefront aberration is related to the transverse aberrations, $\Delta_{\xi'}$, and $\Delta_{\eta'}$, by the formulae $\Delta_\xi = -(R'/n')\,\partial W/\partial X'$ and $\Delta_\eta = -(R'/n')\,\partial W/\partial Y'$

Considering [15] normalised polar coordinates, (ρ',θ'), with $X'/X'_p = \rho'\mathrm{Cos}\theta'$ and $Y/Y'_p = \rho'\mathrm{Sin}\theta'$ (X'_p and Y'_p being coordinates of the marginal rays), the expansion up to order $n_{\max}$ of $W(\rho',\theta')$ in Zernike polynomials of different orders n and angular frequencies m weighed by coefficients C_n^m is [4,15]

$$W(\rho',\theta') = \sum_{n=0}^{n_{\max}} \sum_{m=-n}^{n} C_n^m Z_n^m(\rho',\theta'), \tag{1}$$

with $n+m$ even and $m \leqslant n$. If $R_n^{|m|}(\rho')$ are radial polynomials; $f^m(\theta')$ is such that $f^m(\theta') = \cos(m\theta')$ when $m \geqslant 0$ and $f^m(\theta') = \sin(-m\theta')$ when $m<0$ and if $\delta_{\mathrm{mo}} = 1$ when $m = 0$ and $\delta_{\mathrm{mo}} = 0$ when $m \neq 0$, we have

$$Z_n^m(\rho'\theta') = N_n^m R_n^{|m|}(\rho') f^m(\theta'),$$
$$N_n^m = [2(n+1)/(1+\delta_{\mathrm{mo}})]^{1/2}. \tag{2}$$

2.2. Aberrations and pupil of the eye

In the case of the eye, the coefficients C_n^m (termed C_j in the bar plots with $j = (n(n+2)+m)/2$) [15]) are evaluated using information available from ray tracing. For corneal aberrations, the rays are usually traced numerically [16–19] employing the corneal profile supplied by a topography system and if the keratometric axis is regarded as reference as a starting point, then a change of coordinates to consider the line of sight as reference is recommended [14,15,21]. The root mean square of the total aberration (i.e. of higher and lower order), $\mathrm{RMS_{TOT}}$, is [15]

$$\mathrm{RMS_{TOT}} = \left[\sum_{n=0}^{n_{\max}} \sum_{m=-n}^{n} \left(C_n^m\right)^2\right]^{1/2}. \tag{3}$$

In what follows, the root mean square corresponding to higher-order aberrations ($n>2$ of Eq. (3)) is termed $\mathrm{RMS_{HO}}$ and that corresponding to these aberrations plus the second-order astigmatism is termed RMS.

Higher-order aberrations are affected by pupil size and centring [1,2] and, under natural viewing conditions and if the external conditions are fixed, its diameter, which we denote DP, and the displacement of its centre with respect to corneal vertex, which we denominate $\Delta X'$ and $\Delta Y'$ (along the X'- and Y'-axes, respectively) vary from one subject to another. For a given eye, pupil diameter varies if illumination varies (adaptation), if the illumination of the other eye varies, if the viewing distance varies (accommodatic miosis), if the psychological or physical state of the subject varies; etc. In a previous work [26] we obtained that in normal eyes, under natural viewing conditions and for illuminances at the pupil between 2.5 and 42 lux, pupil diameter varies between 3 and 8 mm depending on the subject and on the illumination and, additionally, if the eye, illumination and viewing distance are fixed, pupil diameter suffers variations which are within 25% of the minimum diameter.

3. Methodology and results

For each eye, using the SN CT 1000 topography system, we obtain the topography and the corneal aberrometry evaluated considering as the origin of the coordinates system the corneal vertex (intersection of the cornea with the keratometric axis when the subject looks at the fixation point). We take into account the data corresponding to DP and decentring $(\Delta X',\Delta Y')$, Zernike coefficients (C_j) and corneal $\mathrm{RMS_{HO}}$ for pupils of diameter DP and 6 mm.

While the topography is captured, the subject has both eyes opened, the ophthalmologic room is illuminated and the eye under study also receives light originated at the topography system. The illuminance at the location of each eye, measured with a photometer IL 1700 of International Light, is in the photopic range and it is $E_{\mathrm{eye\ under\ study}} = (260 \pm 20)$ lux and $E_{\mathrm{other\ eye}} = (90 \pm 10)$ lux.

3.1. Methodology and results for the first group

3.1.1. Methodology

In the first group, we consider 10 normal eyes of five young subjects (two male and three female) and we have

E.C. : 18 years old (no refractive correction required),
E.D.C. : 25 years old (no refractive correction required),
A.C. : 22 years old ($+0.25$ D in the right eye and -1.25 D in the left eye),
M.S. : 18 years old ($+0.75$ D -0.25 D $\times 130^\circ$ in the right eye and $+3$ D 0.5 D $\times 30^\circ$ in the left eye) and
K.B. : 33 years old (-1 D in the right eye and -0.5 D -1.75 D $\times 0^\circ$ in the left eye).

In each eye, five topographic determinations (each indicated by a number N with $N = 1,\ldots 5$) are performed in one experimental session. All the topographies are obtained by the same technician, no topography is captured immediately before or after blinking and the time interval between successive topographies in one eye is $\Delta t = (10.5 \pm 3.6)$ min. For any magnitude u whose mean value is $\langle u \rangle$, the perceptual dispersion of u with respect to the mean is termed $\Delta_{\%} u = 100|u—\langle u \rangle|/\langle u \rangle$.

In Fig. 2, as examples, we show the topography, the morphological and refractive maps and the corneal aberrometry for pupils of diameter DP and 6 mm for the cases $N = 3$, right eye (without astigmatism) of subject E.C and $N = 4$, left eye (with astigmatism) of K.B. In each aberrometry, the OPD maps corresponding to RMS_{HO} (below) and to RMS (above) are shown to the left and the spot diagram and Zernike coefficients to the right.

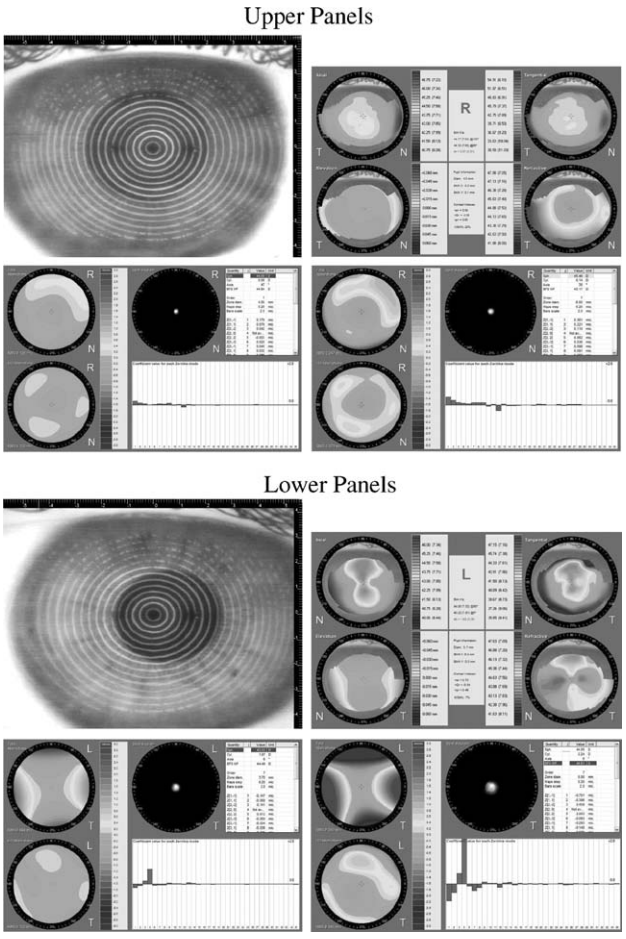

Fig. 2. Topographic and aberrometric results for $N = 3$, right eye of E.C. (four upper panels) and $N = 4$, left eye of K.B. (four lower panels). For each eye we show Placido rings and pupil (above left), morphological and refractive maps (above right) and aberrometries for pupil diameters equal to DP (below left) and 6 mm (below right).

3.1.2. Results for the variation of pupil diameter and centring for each subject and between subjects

The variation undergone by the pupil from one measurement to another for a particular eye can be due to a measurement error or to natural variations [26] and we obtain the results that follows.

(a) *Variations due to measurement errors*: Since pupil contour is not neatly defined in the topography, there is an error in the determination of DP, of $\Delta X'$ and of $\Delta Y'$ and, as an example we do five determinations for the two cases in Fig. 2. For $N = 3$, right eye of E.C., we obtain $DP_{EC} = (4.62 \pm 0.04)$ mm; $\Delta X'_{E.C.} = (-0.18 \pm 0.04)$ mm and $\Delta Y'_{E.C.} = (-0.10 \pm 0.00)$ mm while for $N = 4$, left eye of K.B., we get $DP_{K.B.} = (3.84 \pm 0.05)$ mm; $\Delta X'_{K.B.} = (-0.40 \pm 0.0)$ mm and $\Delta Y'_{K.B.} = (-0.08 \pm 0.04)$ mm. Thus the error in the determination of pupil diameter and decentring is at the most 0.05 mm, so the perceptual error in determining DP is less than 2% and, additionally, we consider the decentring significant if it is larger than 0.1 mm.

(b) *Natural variations*: There are natural variations in pupil size (treated in Section 2.2) that do not constitute measurement errors. In the upper left panel of Fig. 3, we indicate the values of natural pupil diameter, DP, for the five measurements in every eye and, considering each eye, we get $\Delta_{\%}DP < 21\%$. In the upper right panel of Fig. 3, we show the results for the mean value of DP and its standard deviation per eye. Both eyes of the same subject have similar diameters (indicating absence of certain pathologies [1]) and there is a relatively high dispersion of diameters between subjects since we get

$$3 \text{ mm} \leqslant \langle DP \rangle \leqslant 5.3 \text{ mm} \quad (4)$$

Decentring of pupil from corneal vertex (lower left panel of Fig. 3), is such that $|\Delta Y'|$ is negligible and $|\Delta X'| \leqslant 0.2$ mm for all the eyes except for $N = 5$ of the left eye of K.B., which is such that $|\Delta X'|$ reaches 0.6 mm which is 15% of DP (in this case DP = 3.9 mm). For every measurement of every subject except for $N = 5$ right eye of M.S. for which $\Delta X' = 0.1$ mm that is of the

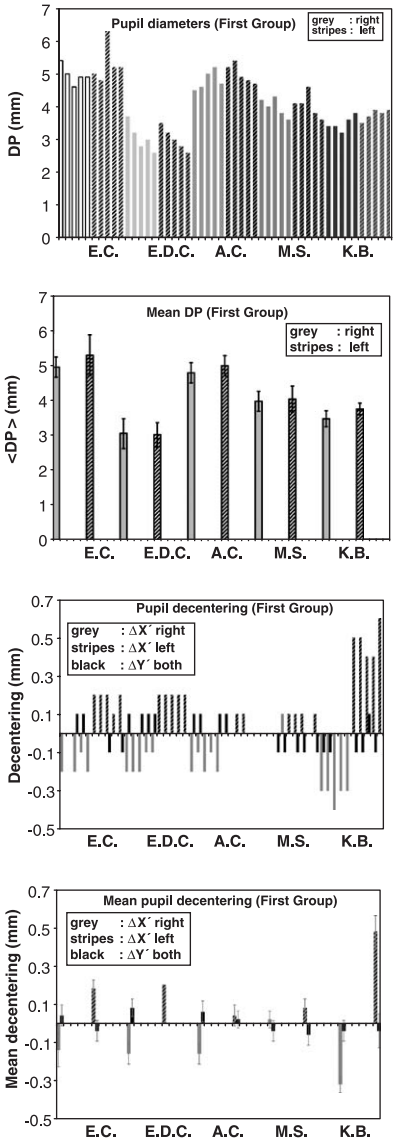

Fig. 3. Size and centring of the pupil for the first group. Upper panels (grey: right eye; stripes: left eye): DP in the five measurements of each eye (left) and mean value of DP for each eye (right). Lower panels (grey: $\Delta X'$ for the right eye, stripes: $\Delta X'$ for the left eye; black: $\Delta Y'$ for both eyes): pupil decentring from corneal vertex in the five measurements of each eye (left) and mean value of decentring for each eye (right)

order of magnitude of measurement error, we get

$$\begin{aligned}&\text{Right eye}: \quad \Delta X' \leqslant 0 \quad \Delta Y' \text{ small},\\ &\text{Left eye}: \quad \Delta X' \geqslant 0 \quad \Delta Y' \text{ small}.\end{aligned} \tag{5}$$

Therefore in both eyes of the five normal young subjects of the first group, pupil centre is displaced towards the temporal region with respect to corneal vertex (this can be seen in Fig. 3 for K.B.).

3.1.3. Results for RMS_{HO} and RMS (pupil diameter 6 mm and DP)

For each eye, we evaluate the aberrations for DP and for a fixed pupil diameter of 6 mm (associated magnitudes are indicated with supra-indices (DP) and (6 mm) respectively). In the two upper panels of Fig. 4 we plot RMS_{HO} for the five measurements of the right eye (black) and the left eye (stripes) of each subject and also RMS for both eyes (grey). When pupil diameter is the natural one (left panel), for each particular eye, $RMS_{HO}^{(DP)}$ and $RMS^{(DP)}$ vary considerably from one measurement to another (principally because DP varies) and the corresponding perceptual dispersion is $\Delta_{\%}RMS_{HO}^{(DP)} < 93\%$ and $\Delta_{\%}RMS^{(DP)} < 75\%$. Contrarily, when pupil diameter is 6 mm (right panel), the variation of $RMS_{HO}^{(6\ mm)}$ and $RMS^{(6\,mm)}$ in the five measurements of an eye is small, an adequate repeatability being attained. We obtain $\Delta_{\%}RMS_{HO}^{(6\ mm)} < 26\%$ and $\Delta_{\%}RMS^{(6\,mm)} < 19\%$ except for $N = 1$ in the left eye of A.C. who, because of fatigue, was probably not in an optimum condition and has $\Delta_{\%}RMS_{HO}^{(6\ mm)} = 58\%$ and $\Delta_{\%}RMS^{(6\,mm)} = 55\%$. Averaging the mean values of all the eyes, it results in

$$\left\langle\left\langle RMS_{HO}^{(6\ mm)}\right\rangle\right\rangle = (0.37 \pm 0.06)\ \mu m \tag{6}$$

Hence, for a 6 mm pupil, the dispersion of RMS_{HO} among normal young subjects is smaller than for the natural pupil size and, since 6 mm is usually larger than natural pupil diameters under photopic conditions, the values of $RMS_{HO}^{(6\ mm)}$ are usually larger than those of $RMS_{HO}^{(DP)}$ ($\left\langle\left\langle RMS_{HO}^{(6\ mm)}\right\rangle\right\rangle$ can be up to eight times greater than $\left\langle RMS_{HO}^{(DP)}\right\rangle$). In the lower left panel of Fig. 4, to facilitate comparison, we plot the mean values of RMS_{HO} for each eye for pupils of diameter DP and 6 mm. We have

$$\begin{aligned}&0.05\ \mu m \leqslant \left\langle RMS_{HO}^{DP}\right\rangle \leqslant 0.19\ \mu m,\\ &0.30\ \mu m \leqslant \left\langle RMS_{HO}^{(6\ mm)}\right\rangle \leqslant 0.51\ \mu m.\end{aligned} \tag{7}$$

Furthermore, comparing RMS with RMS_{HO}, the second-order corneal astigmatism for pupil of diameter DP (left upper panel of Fig. 4) is negligible in all eyes except for the right eye of A.C. and the left eye of M.S. (moderate astigmatism) and for both eyes of K.B. (astigmatism is the dominant aberration).

3.1.4. Results for the fourth-order spherical aberration

Spherical aberration is an important corneal aberration in all the considered eyes. In the lower right panel of Fig. 4, we indicate the values of the spherical aberration coefficients yielded by the topography system (coordinates origin at corneal vertex) for a 6 mm pupil. We consider each eye measurement and also a spherical surface of radius equal to the apical one

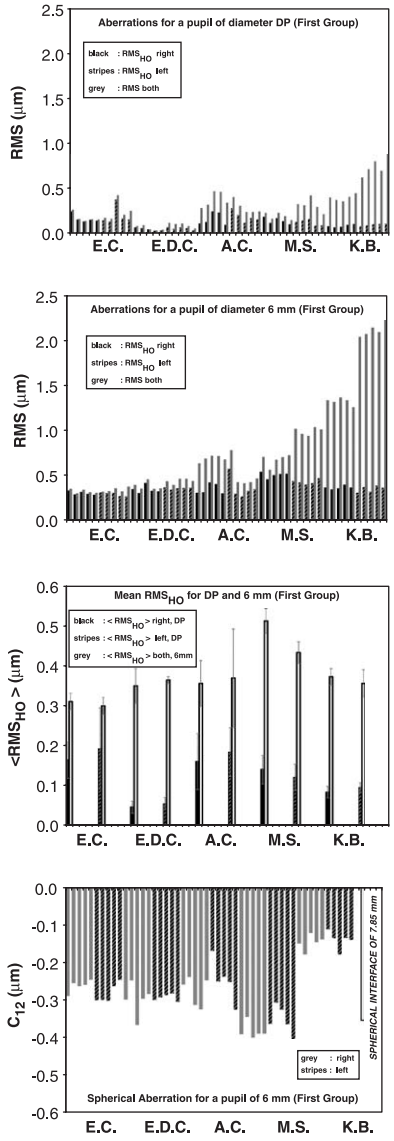

Fig. 4. Corneal aberrations for the first group. Upper panels (black: RMS_{HO} right eye; stripes: RMS_{HO} left eye; grey: RMS both eyes): RMS_{HO} and RMS for every measurement for natural pupil (left) and 6 mm pupil (right). Lower left panel (black: $RMS_{HO}^{(DP)}$ right eye; stripes: $RMS_{HO}^{(DP)}$ left eye; white with black border: $RMS_{HO}^{(6\,mm)}$: comparison between the mean values of $RMS_{HO}^{(DP)}$ and $RMS_{HO}^{(6\,mm)}$. Lower right panel: spherical aberration for 6 mm pupil for the five measurements of the right eye (grey) and the left eye (stripes) of each subject

(R_{apical}-7.85 mm) which is C_{12} (sphere) $= -0.36\,\mu m$. We obtain $0.11\,\mu m < |C12| < 0.40\,\mu m$ and considering the mean values per eye, the maximum is $(0.38 \pm 0.02)\,\mu m$ which is similar to C_{12}(sphere). Taking into account these and other results [21], for a 6 mm pupil, a corneal spherical aberration of up to 0.4 μm can be considered as normal and, moreover, it is probably compensated up to a high degree by that originated in the internal optics of the eye [11,19,21].

On the other hand, if a spherical aberration coefficient $C_{12}^{(DA)}$ is determined regarding the coordinates origin at the corneal vertex and an artificial pupil of diameter DA, then when a pupil of diameter DP centred at the real pupil centre is considered, spherical aberration introduces (besides lower-order aberrations) both spherical aberration and coma. As an example, we analyse the case $N = 4$, left eye of K.B. (Fig. 2) which has relatively low coma and spherical aberration and large decentration since $DP = 3.7\,mm$, $C_8^{(DP)} = -0.04\,\mu m$, $C_8^{(6\,mm)} = -0.15\,\mu m$, $C_{12}^{(DP)} = -0.02\,\mu m$, $C_{12}^{(6\,mm)} = -0.14\,\mu m$ and $\Delta X' = 0.5\,mm$.For $DA = 6\,mm$ and aberrations computed with origin at the pupil centre, the spherical aberration and coma coefficients (ignoring other higher order aberrations), $C_{12}^{(DP)}$ and $C'^{(DP)}_8$, are $C'^{(DP)}_{12} = C_{12}^{(6\,mm)}\,(DP/DA)^4 = -0.02\,\mu m$ and $C'^{(DP)}_8 = C_8^{(6\,mm)}(DP/DA)^3 + C_{12}^{(6\,mm)}\ 2\ (10)^{1/2}\ (2\ \Delta X'\ DP^3/DA^4) = (-0.04 - 0.03)\,\mu m = -0.07\,\mu m$ so, since the pupil-centred spherical aberration coefficient is independent of $\Delta X'$, $C_{12}^{(DP)}$, is equal to $C_{12}^{(DP)}$ while since spherical aberration gives rise to coma, the pupil-centred coma coefficient, $C'^{(DP)}_8$, is considerably larger than $C_8^{(DP)}$. In eyes with higher values of $C_{12}^{(6\,mm)}$ and/or DP and/or $\Delta X'$, the spherical aberration and coma coefficients resulting from the translation and contraction of the pupil increase and, though the general calculation is recommended [14,15], it is beyond the scope of the present study.

3.2. Second group of eyes

In this group we consider 24 eyes with different pathologies of 12 subjects (age between 25 and 68 years) and we obtain only one topography and aberrometry per eye (24 measurements). The subjects, sorted in each pathology according to increasing RMS_{HO}, are

Normal (1.25 to +6 D sphere; 0 to −0.5 D cylinder): R.E. (51 years old) and S.C. (52 years old),

Astigmatism (−5.5 to +3.25 D sphere; −1.5 to −4.5 D cylinder): J.B. (25 years old), M.F. (29 years old), A.L. (68 years old), S.B. (43 years old),

Post-refractive surgery (+0.5 to +3.5 D sphere; −0.5 to −4 D cylinder): G.A. (37 years old), V.C. (40 years old), C.F. (49 years old)

Keratoconus, (−9.5 to +1 D sphere; −1 to −4.5 D cylinder): L.V. (40 years old), M.D. (30 years old), G.F. (30 years old).

3.2.1. Results for pupil diameter and centring

Concerning pupil diameter (left panel of Fig. 5), similar to the first group, we get

$$2.7\,mm \leqslant DP \leqslant 5.6\,mm. \quad (8)$$

Regarding decentring (right panel of Fig. 5), in cases of keratoconus (last three subjects of Fig. 5), an upward displacement of the pupil centre from corneal

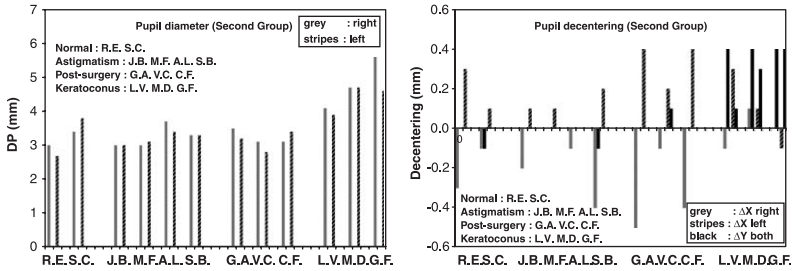

Fig. 5. Results for the second group. Left panel (grey: right eye; stripes: left eye): DP for each subject. Right panel (grey: $\Delta X'$ right eye; stripes: $\Delta X'$ left eye; black: $\Delta Y'$ both eyes): pupil decentring with respect to corneal vertex.

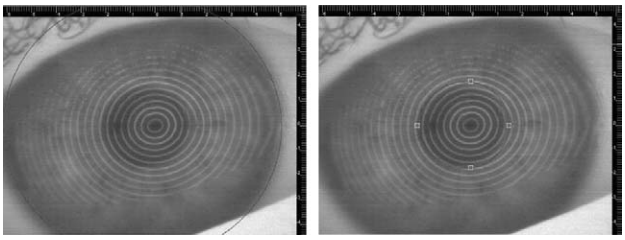

Fig. 6. Displacement from corneal vertex of the iris centre (left panel) and of the pupil centre (right panel) for right eye of S.B.

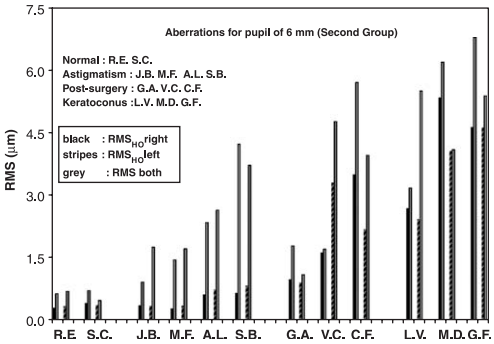

Fig. 7. Aberrations for a 6 mm pupil (second group; black: RMS_{HO} right eye; stripes: RMS_{HO} left eye; grey: RMS both eyes).

vertex often dominates and $\Delta Y' \leqslant 0.4\,\text{mm}$ while in the other cases, as in the first group, the displacements that are significant are towards the temporal region. On the other hand, Adler [1] states that the pupil centre is placed in a location slightly inferior and nasal with respect to the centre of the cornea. To study whether this statement is compatible with our findings and considering normal or astigmatic eyes (which are such that vertical displacements are negligible), besides the displacement of the pupil centre from corneal vertex ($\Delta X'$), we take into account the displacement of the curvature centre of the exterior iris border from corneal vertex ($\Delta X'_{\text{IRIS}}$). As an example, in Fig. 6 we show the case of the right eye of subject S.B. and we obtain $\Delta X' = -0.3\,\text{mm}$ and $\Delta X'_{\text{IRIS}} = -0.5\,\text{mm}$ so the displacement of the pupil centre from the iris centre is 0.2 cm, this is, as Adler states, towards the nasal region. This result is usually verified in the normal or astigmatic eyes considered in the present article.

3.2.2. Results for RMS_{HO} and RMS (pupil diameter 6 mm)

Only considering a 6 mm pupil (Fig. 7 which is such that the maximum value along the axis is 7.5 μm instead of 2.5 μm as in Fig. 4), while in normal eyes RMS_{HO} is at the most 0.4 μm (as in the first group), in cases of keratoconus it reaches 5.3 μm and we obtain:

$$\begin{aligned}
&0.3\,\mu\text{m} \leqslant \text{RMS}_{\text{HO}}^{(6\,\text{mm})} \leqslant 0.4\,\mu\text{m for normal eyes,}\\
&0.3\,\mu\text{m} \leqslant \text{RMS}_{\text{HO}}^{(6\,\text{mm})} \leqslant 0.8\,\mu\text{m for astigmatism,}\\
&0.9\,\mu\text{m} \leqslant \text{RMS}_{\text{HO}}^{(6\,\text{mm})} \leqslant 3.5\,\mu\text{m for post-surgery,}\\
&2.4\,\mu\text{m} \leqslant \text{RMS}_{\text{HO}}^{(6\,\text{mm})} \leqslant 5.3\,\mu\text{m for keratoconus.}
\end{aligned} \tag{9}$$

4. Conclusion

Considering two groups of subjects, we analyse pupil and aberration data supplied by the SN CT 1000 topography system. For the first group (10 young normal eyes), we perform five measurements per eye and study repeatability. We take into account two different pupil sizes, a natural one and a fixed value of 6 mm and the corresponding values of RMS_{HO}. Fourth-order spherical aberration is an important corneal aberration in all the eyes of this group and, for a 6 mm pupil, its maximum value is $(-0.38 \pm 0.02)\,\mu\text{m}$ which is in the range reported in other studies for normal corneas [21]. For the second group (four normal adult eyes, eight with astigmatism, six with post-refractive surgery and six with keratoconus) we perform

only one measurement per eye. We obtain the following general conclusions:

(a) *Repeatibility of pupil size and centring in successive measurements for one eye*: For the first group, in the successive measurements of the natural pupil diameter of a given eye, we obtain a perceptual dispersion smaller than 21% which is consistent with natural pupil size variations previously found [26].
(b) *Variation of pupil diameter between subjects*: For an illumination of (260 ± 20) lux at the eye under study and (90 ± 10) lux at the other eye, the natural pupil diameters have a significant dispersion between eyes ranging from 3 to 5.3 mm in the first group and from 2.7 to 5.6 mm in the second group.
(c) *Pupil decentering*: The decentering values which we obtain are in the range reported in other works [19] and, additionally, our results reveal a displacement of pupil centre from corneal vertex of up to 0.5 mm towards the temporal region, except for the six eyes with keratoconus where an upwards displacement of up to 0.4 mm can dominate. Moreover, in normal or astigmatic eyes, the displacement of the pupil centre from the curvature centre of the iris exterior border usually results to be towards the nasal region.
(d) *Dispersion of RMS_{HO} for a 6 mm pupil*: Considering a fictitious pupil of 6 mm, for the first group there is little perceptual dispersion both for a particular eye and between eyes, and the average across all eyes is (0.37 ± 0.06) μm. The relatively low deviation with respect to the average reveals, on the one hand, the adequacy of the measurement methodology and, on the other hand, that normal young eyes have similar RMS_{HO} when the same pupil size is considered in all of them. Contrarily and as expected, for the second group the dispersion increases significantly since RMS_{HO} is between 0.3 μm (normal eye) and 5.3 μm (keratoconus). Our results are consistent with recent reports of other authors. For example, Applegate et al. [17], considering 13 normal patients and 78 patients with various corneal conditions, obtained that, for a 7 mm pupil, RMS_{HO} is around 0.5 μm in normal corneas and between 2 and 5.5 μm in those suffering from keratoconus. Marcos et al. [21], considering 14 myopic eyes (age 28.9 ± 5.4 years), found that for a 6.5 mm pupil and for corneal aberrations, RMS_{HO} before LASIK is between 0.2 and 1.1 μm and it increases after LASIK, the maximum being 3 μm.
(e) *Dispersion of RMS_{HO} for a natural pupil*: For the first group, the RMS_{HO} value obtained for a 6 mm pupil significantly decreases (except for a few eyes with naturally large pupils where the decrease is moderate) when the natural pupil corresponding to photopic illumination is considered and the dispersion between eyes increases, the mean value per eye ranging from 0.05 μm to 0.19 μm.

The results show the consistency of the data supplied by the SN CT 1000 system, the convenience of capturing various topographies per eye principally to account for changes in the subject's psycho-physical state and the importance of considering the natural pupil diameter when aberrations are determined to give insight about everyday visual performance. Finally, since the SN CT 1000 software evaluates aberrations with origin at the videokeratography map centre, to describe image formation through the cornea with higher accuracy, aberration coefficients should be recalculated correcting the decentration between the corneal vertex and pupil centre.

Acknowledgements

This work was carried out with the support of Universidad de Buenos Aires and Consejo Nacional de Investigaciones Científicas y Técnicas. We are grateful to Mr. Ezequiel Carbón for drawing the figures.

References

[1] P. Kaufman, y.A. Alm, Adler fisiología del ojo, Elsevier, Madrid, 2004.
[2] D.D. Michaels, Visual Optics and Refraction, A Clinical Approach, C. V. Mosby, St. Louis, 1980.
[3] J.W. Goodman, Introduction to Fourier Optics, Mc Graw-Hill, New York, 1996.
[4] M. Born, B. Wolf, Principles of Optics, Pergamon, Oxford, 1987.
[5] H.H. Hopkins, Image formation by a general optical system. 1. General theory, Appl. Opt. 24 (1985) 2491–2505.
[6] S.A. Comastri, J.M. Simon, Ray tracing, aberration function and spatial frequencies, Optik 66 (1984) 175–190.
[7] J.M. Simon, S.A. Comastri, Image forming systems: matrix formulation of the optical invariant via Fourier optics, J. Mod. Opt. 43 (1996) 2533–2541.
[8] S.A. Comastri, J.M. Simon, R. Blendowske, Generalized sine condition for image-forming systems with centering errors, J. Opt. Soc. Am. A 16 (1999) 602–611.
[9] J. Liang, D.R. Williams, D.T. Miller, Supernormal vision and high-resolution retinal imaging through adaptive optics, J. Opt. Soc. Am. A 14 (1997) 2884–2892.
[10] J. Liang, D.R. Williams, Aberrations and retinal image quality of the normal human eye, J. Opt. Soc. Am. A 14 (1997) 2873–2883.
[11] P. Artal, A. Guirao, Contribution of the cornea and the lens to the aberrations of the human eye, Opt. Lett. 23 (1998) 1713–1715.
[12] A. Guirao, C. Gonzalez, M. Redondo, E. Geragbty, S. Norrby, P. Artal, Average optical performance of the

human eye as a function of age in a normal population, Inv. Opt. Vis. Sci. 40 (1999) 203–213.
[13] A. Guirao, D.R. Williams, I.G. Cox, Effect of rotation and translation on the expected benefit of an ideal method to correct the eye's higher order aberrations, J. Opt. Soc. Am. A 18 (2001) 1003–1015.
[14] R. Applegate, L. Thibos, A. Bradley, S. Marcos, A. Roorda, T. Salmon, D. Atchison, Reference axis selection: subcommittee report of the OSA working group to establish standards for measurement and reporting of optical aberrations of the eye, J. Refract. Surg. 16 (2000) 656–658.
[15] L. Thibos, R. Applegate, J. Schwiegerling, R. Webb, VST Members, Standards for reporting the optical aberrations of eyes, Vis. Sci. Appl. Tops Volume (2000) 35.
[16] A. Guirao, P. Artal, Corneal wave aberration from videokeratography: accuracy and limitations of the procedure, J. Opt. Soc. Am. A 17 (2000) 955–965.
[17] R. Applegate, G. Hilmantel, H. Howland, E. Tu, T. Starck, J. Zayac, Corneal first surface optical aberrations and visual performance, J. Refract. Surg. 16 (2000) 507–514.
[18] R. Applegate, H. Howland, S. Klyce, Corneal aberrations and refractive surgery. Customized Corneal Ablation: The Quest for Supervision, Slack Incorporated, USA, 2001.
[19] S. Barbero, S. Marcos, J. Merayo-Lloves, E. Moreno Barriuso, Validation of the Estimation of Corneal Aberrations From Videokeratography in Keratoconus, J. Refract. Surg. 18 (2002) 263–269.
[20] S. Marcos, Aberrations and visual performance following standard laser vision correction, J. Refract. Surg. 17 (2001) 596–601.
[21] S. Marcos, S. Barbero, L. Llorente, J. Merayo-Lloves, Optical response to myopic LASIK surgery from total and corneal aberration measurements, Inv. Ophthalmol. Vis. Sci. 42 (2001) 3349–3356.
[22] E. Moreno Barriuso, S. Marcos, R. Navarro, S. Burns, Comparing laser ray tracing, the spatially resolved refractometer and the Hartmann–Shack sensor to measure the ocular wave aberration, Optom. Vis. Sci. 78 (2001) 152–156.
[23] T.O. Salmon, R.W. West, W. Gasser, T. Kenmore, Measurement of refractive errors in young miopes using the COAS Shack–Hartmann aberrometer, Optom. Vis. Sci. 80 (2003) 6–14.
[24] R. Navarro, O. Nestares, B. Antona, y J. Hernandez, Predicting visual acuity from measured ocular aberrations, Meeting of the International Commission for Optics, Italy, Proc. SPIE 4829 (2002) 971–972.
[25] R. Navarro, P. Rodriguez, L. Gonzalez, J. Aporta, J. L. Hdez-Matamoros, Ray tracing in the human eye: measurement and modeling of optical aberrations. 5th Iberoamerican Meeting on Optics and 8th Latin American Meeting on Optics, Lasers and Their Applications, Venezuela, Proc. SPIE 5622 (2004) 113–118.
[26] S.A. Comastri, R. Echarri, T. Pfortner, Correlation between visual acuity and pupil size, 5th Iberoamerican Meeting on Optics and the 8th Latin American Meeting of Optics, Lasers and Their Applications, Venezuela, Proc. SPIE 5622 (2004) 1341–1346.
[27] L. Gonzalez, R. Navarro, H. L. Hdez Matamoros, Efficient numerical modeling of the cornea and applications, 5th Iberoamerican Meeting on Optics and 8th Latin American Meeting on Optics, Lasers and their Applications, Venezuela, Proc. SPIE 5622 (2004)119–125.
[28] H. Guo, Z. Wang, Q. Zhao, W. Quan, Y. Wang, Individual eye model based on wavefront aberration, Optik 116 (2005) 80–85.
[29] H. Hofer, L. Chen, G.Y. Yoon, B. Singer, Y. Yamauchi, D. Williams, Improvement in retinal image quality with dynamic correction of the eye's aberrations, Opt. Express 8 (2001) 631–643.